

UC Davis

UC Davis Previously Published Works

Title

Unique Hydrogen Bonding of Adenine with the Oxidatively Damaged Base 8-Oxoguanine Enables Specific Recognition and Repair by DNA Glycosylase MutY

Permalink

<https://escholarship.org/uc/item/57v404vd>

Journal

Journal of the American Chemical Society, 142(48)

ISSN

0002-7863

Authors

Majumdar, Chandrima
McKibbin, Paige L
Krajewski, Allison E
[et al.](#)

Publication Date

2020-12-02

DOI

10.1021/jacs.0c06767

Peer reviewed



Published in final edited form as:

J Am Chem Soc. 2020 December 02; 142(48): 20340–20350. doi:10.1021/jacs.0c06767.

Unique Hydrogen-Bonding of Adenine with the Oxidatively Damaged Base 8-oxoguanine Enables Specific Recognition and Repair by DNA Glycosylase MutY

Chandrima Majumdar[†], Paige L. McKibbin[†], Allison E. Krajewski[‡], Amelia H. Manlove[†], Jeehiun K. Lee^{‡,*}, Sheila S. David^{†,*}

[†]Department of Chemistry, University of California Davis, Davis, CA 95616, USA

[‡]Department of Chemistry and Chemical Biology, Rutgers, The State University of New Jersey, New Brunswick, New Jersey 08854, USA

Abstract

The DNA glycosylase MutY prevents deleterious mutations resulting from guanine oxidation by recognition and removal of adenine (A) misincorporated opposite 8-oxo-7,8-dihydroguanine (OG). Correct identification of OG:A is crucial to prevent improper and detrimental MutY adenine excision from G:A or T:A base pairs. Here we present a structure-activity relationship (SAR) study using analogs of A to probe the basis for OG:A specificity of MutY. We correlate observed *in vitro* MutY activity on A analog substrates with their experimental and calculated acidities to provide mechanistic insight into the factors influencing MutY base excision efficiency. These data show that H-bonding and electrostatic interactions of the base within the MutY active site modulate the lability of the *N*-glycosidic bond. A analogs that were not excised from duplex DNA as efficiently as predicted by calculations provided insight into other required structural features, such as steric fit and H-bonding within the active site for proper alignment with MutY catalytic residues. We also determined MutY-mediated repair of A analogs paired with OG within the context of a DNA plasmid in bacteria. Remarkably, the magnitudes of decreased *in vitro* MutY excision rates with different A analog duplexes do not correlate with the impact on overall MutY-mediated repair. The feature that most strongly correlated with facile cellular repair was the ability of the A analogs to H-bond with the Hoogsteen face of OG. Notably, base-pairing of A with OG uniquely positions the 2-amino group of OG in the major groove and provides a means to indirectly select only these inappropriately placed adenines for excision. This highlights the importance of OG lesion detection for efficient MutY-mediated cellular repair. The A analog SAR also highlight the types of modifications tolerated by MutY and will guide the development of specific probes and inhibitors of MutY.

Graphical Abstract

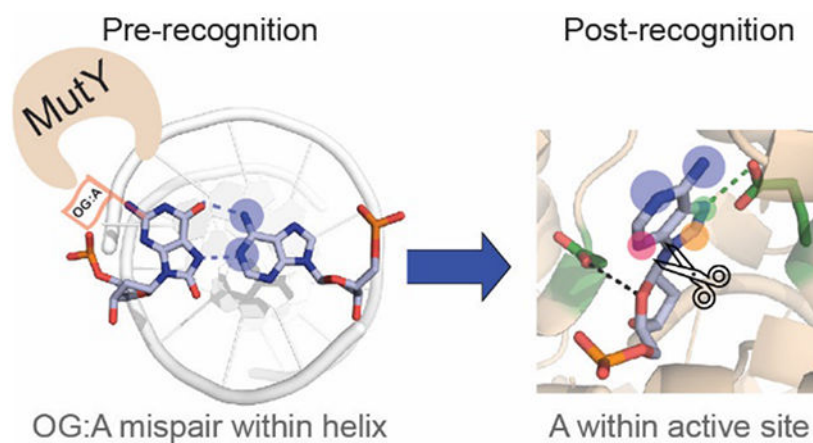
*Corresponding Authors ssdavid@ucdavis.edu (S.S.D.); jeehiun@chem.rutgers.edu (J.K.L.).
Author Contributions

All authors have reviewed and approved the final version of this manuscript.

ASSOCIATED CONTENT

This material is available free of charge via the Internet at <http://pubs.acs.org>.

- Materials and methods, binding titrations, figures S1-S8, structures and cartesian coordinates of the adenine analogs



Keywords

DNA repair; MutY; Mutyh; adenine glycosylase; 8-oxoguanine; structure-activity relationship

INTRODUCTION

Despite being the repository of genetic information and the instruction manual for cells, DNA is a dynamic molecule susceptible to modification via a variety of chemical reactions.¹ Modifications of DNA nucleobases due to reactions with alkylating agents and reactive oxygen and nitrogen species (RONS) often alter coding properties that leads to deleterious mutations.²⁻⁶ Exposure to RONS creates a wide variety of oxidized DNA nucleobases, of which 8-oxo-7,8-dihydroguanine (OG) is one of the most common.^{7,8} While OG retains the overall structure of guanine (G) and can base pair (bp) to cytosine (C), the presence of the 8-oxo group and the concomitant protonation of N7 creates a thymine (T)-like Hoogsteen base pairing face that enables formation of a stable bp with adenine (A).⁴ During DNA replication, OG displays its T-like face to the incoming 2'-deoxyribonucleotide triphosphate resulting in misincorporation of A by replicative polymerases and formation of an OG:A mismatch.^{9,10} The situation is further exacerbated by the more efficient extension of OG:A termini compared to OG:C by mammalian DNA polymerases that leads to the persistence of these promutagenic mismatches in DNA.^{11,12} As a result, the presence of OG in the genome promotes the accumulation of G:C to T:A mutations (Figure 1).

The 'GO repair pathway' in bacteria is responsible for protecting DNA from mutations associated with OG.¹³ The key base excision repair (BER) glycosylases involved in this pathway are Fpg and MutY. MutY removes the undamaged A from OG:A mismatches.¹⁴ Subsequently, downstream repair enzymes reinstate C opposite OG, providing a proper substrate for Fpg removal of OG from OG:C bps (Figure 1).¹⁵ The importance of prevention of mutations associated with OG is highlighted by the presences of OG repair pathways in all domains of life.¹⁵⁻¹⁷ In humans, inheritance of functionally deficient variants of the homolog MUTYH have been linked to a colorectal cancer predisposition syndrome known as MUTYH-associated polyposis (MAP).^{16,18,19} The Leiden Open Variant Database (LOVD) reports over 300 different MAP related mutations in the *MUTYH* gene. Many

MAP mutations result in amino acid variants within the N-terminal catalytic domain and C-terminal OG recognition domain, indicating the importance of MUTYH function for genome maintenance.¹⁷

Mechanistic studies on MutY, including kinetic isotope effects (KIE), predicted an S_N1 hydrolytic base excision mechanism involving N7 protonation and formation of an oxacarbenium ion transition state and intermediate.^{20,21} Subsequent crystallographic studies of *Geobacillus stearothermophilus* (*Gs*) MutY bound to an azaribose transition state mimic indicated approach of the water nucleophile from the same side as the departing adenine base; this structural inference was supported by MutY-catalyzed methanolysis studies that showed retention of configuration at C1' consistent with a two-step mechanism for A excision.²² In a proposed revised mechanism, A is protonated by *Gs* MutY Glu43 at N7 to facilitate its departure leading to formation of a transient oxacarbenium ion stabilized as a covalent intermediate with Asp144.²² In a second step, Glu43 activates a water nucleophile to hydrolyze the acetal intermediate to form the abasic site product (Figure 2a).²² The resulting OG:abasic (AP) site product is processed by downstream BER enzymes to restore the originally coded G:C base pair (bp) (Figure 1).

Crystallographic studies have been instrumental in revealing key interactions between the enzyme and its substrate.^{4,15} In the structure of *Gs* MutY bound to a non-cleavable substrate analog OG:FA (FA: *arabino*-2'-fluoro-2'-deoxyadenosine), OG has rotated from the *syn* to *anti* conformation and the A is flipped out of the helix for insertion into the active site (Figure 2b). Within the active site, H-bonding contacts align the A with the catalytic Glu and Asp residues (Glu43 and Asp144 in *Gs* MutY, Glu37 and Asp138 in *Ec* MutY) orienting it for cleavage (Figure 2c).²³ Russelburg *et al.* demonstrated that a C-terminal domain Ser (308 in *Gs* MutY), which forms an H-bond with the N7-H in OG disengages from the N7 lone pair in the corresponding structure with G, suggesting one potential mechanism for discrimination between OG and G.²⁴ Additionally, Wang *et al.* have reported a co-crystal structure of MutY bound to its 'anti-substrate' OG:C, wherein the entry of C into the active site is blocked to prevent accidental and promutagenic excision.²⁵ While these studies provide a wealth of information on features of catalysis after recognition of the lesion, the structures themselves only provide snapshots of late steps in the MutY recognition and excision process, and not the complete series of events that occurred prior to lesion engagement.

In previous studies directed at understanding the structural requirements of OG on lesion recognition and catalysis, we showed that MutY relies on the exocyclic 2-amino group of OG to identify and distinguish this mispair from structurally similar T:A bps.^{26,27} We also showed that OG binding induces conformational changes that influence A excision.^{26,28} Herein, we use structure-activity relationships (SAR) to identify the structural features of A that influence OG:A recognition, verification, base excision and overall cellular repair. The interpretation of these results was aided by calculations of acidity and proton affinities to identify structural features that alter intrinsic lability of the *N*-glycosidic linkage, and how such features may be modulated by electronic and steric interactions within the MutY active site. Factors that influence efficient cellular repair relative to *in vitro* activity suggest that MutY recognizes and detects the misplaced A within OG:A mismatches by virtue of its

ability to uniquely base pair with the *syn* conformer of OG. Once placed within the active site of MutY, the structure of A is further validated through contacts within the active site leading to preferred excision of A and prevention of inaccurate excision of other bases.

RESULTS AND DISCUSSION

Selection of adenine analogs

We selected a series of 8 analogs (Figure 2d) to reveal features of MutY mediated recognition and base excision (Table 1). Calculations were used to assess acidities and proton affinities to evaluate features that impact the lability of the *N*-glycosidic bond of the nucleotide analogs. Duplex stability assays were used to evaluate the impact of the structural changes on base pairing to OG. The consequences of altered structural features on efficiency of MutY glycosylase activity and binding affinity was determined *in vitro* using 30 bp DNA duplexes. The overall impact of MutY-mediated repair in a cellular context was evaluated using the analogs incorporated within a DNA plasmid.

Among the analogs studied, purine (P) lacks the 6-amino group and tests the effect of losing H-bonding to OG_{*syn*} within DNA and within the active site; 2-oxoadenine (2OA) tests the effect of reversal of polarity of the H-bond at N1, whereas inosine (I) represents the complete reversal of H-bonding polarity at N1 and C6. Notably, 2OA may present an alternative cytosine-like Watson-Crick (W-C) face (2OA-cyto) that is protonated at N3 rather than N1 (Figure 3). 6-methyladenine (6mA) is expected to base pair naturally with OG_{*syn*}, however it may experience steric hinderance within the active site due to the N⁶-methyl group. 8-bromo adenine (BA), 7-deaza-8-azadenine (ADA) and 3-deazadenine (Z3) retain the W-C face of A, and therefore maintain the ability to base pair to OG_{*syn*} within the DNA duplex. Z3 has the subtle modification of N3 removal, whereas BA and ADA have altered Hoogsteen faces. ADA is expected to be a poor substrate due to the lack of the N7 required for catalysis. Meanwhile, BA is expected to be a competent mimic bromo substituent may increase the preference for the *syn* conformer and hinder proper engagement within the active site. 2-aminopurine (2AP) tests the importance of the exocyclic 6-amino group of A by shifting it to C2, while still retaining H-bonding to OG. Structural alterations of A are also expected to alter the intrinsic lability of the *N*-glycosidic bond; for example, BA would be anticipated to be more labile to depurination due to the electronegative Br, while Z3 would be less labile, due to the replacement of N with C. Collectively, the analogs used in this study were designed to glean insights into the recognition and repair process by MutY.

MutY has high affinity for adenine analogs paired with OG

The impact of modified A analogs (represented as Y) on mismatch affinity were gauged by measurements of the dissociation constant K_D of the catalytically inactive Glu37Ser MutY variant with a 30 bp OG:Y duplex using electrophoretic mobility shift assays (EMSA). For all tested analogs, the apparent K_D for the Glu37Ser MutY-OG:Y complex was near or below the 0.005 nM limit of detection, indicating tight substrate binding regardless of the A analog paired to OG (Table 1, Figure S1). These results are remarkably different than the impact of OG structural modifications that lead to significantly decreased affinity of MutY.²⁶ Additionally, binding affinities suggest that engagement of the correct base (OG

or A) aids in the MutY recognition of the base pair partner. Specifically, MutY binds to an OG:A duplex at least four orders of magnitude more tightly ($K_D < 0.005$ nM) than an OG:C duplex ($K_D = 44 \pm 21$ nM).³⁰ In turn, the OG:C duplex is bound tighter than a non-specific G:C duplex ($K_D = 150 \pm 60$ nM).³¹ Notably, this is consistent with previous work in our laboratory demonstrating that substitutions of A are more readily tolerated when paired with OG compared to G, highlighting the importance of OG for high affinity with MutY.³⁰⁻³²

***In vitro* MutY-mediated excision of Adenine analogs opposite OG in a 30-bp DNA duplex**

Base excision rate constants (k_2) were determined using a glycosylase assay with WT MutY and a 30 bp OG:Y containing duplex under conditions of single turnover (STO, [MutY] > [DNA]) (Figure 4a, b).^{33,34} While WT MutY was able to excise A from OG:A mispairs with a k_2 of 12 ± 2 min⁻¹, none of the analogs were excised as efficiently, and k_2 values were decreased by 2-fold to 1000-fold (Table 1). Notably, most of the OG:Y substrates were completely converted to product during the hour-long experiments, with the exception of the slowest analog, I (Figure 4c, Table 1). Two of the A analogs, ADA and BA, were found to be minimally excised in 1 hour. However, upon extending the incubation time to 24 h, MutY mediated cleavage of these analogs was observed (Figure S3). We estimated an upper limit of k_2 for OG:BA as 0.007 min⁻¹ and for OG:ADA as 0.002 min⁻¹ based on the extent of product formation in 1 h. The rate constants k_3 relating to product release determined under multiple-turnover (MTO) conditions, were similar to the natural OG:A substrate (0.002 ± 0.001 min⁻¹) for analog substrates that exhibit analogous “burst” kinetics behavior. This finding was not unexpected since base excision results in the formation of the same OG:AP site product in all cases. The analogs 2AP and I were processed inefficiently, and a defined burst phase was not observed and therefore the rate of product release k_3 could not be determined in these experiments (Table 1, Figure 4b, c).³⁴

Acid-catalyzed hydrolysis of A analogs from ssDNA

Since base excision by MutY involves protonation of N7 of A, we expected that the susceptibility of an A analog to acid-catalyzed depurination would impact the efficiency of MutY-catalyzed base excision. We determined the relative extent of acid-catalyzed depurination of the analogs from ssDNA in aqueous solution (Table S1). These experiments revealed that P, 2OA and 2AP are more acid labile than A, whereas 6mA, BA and I are similar to A. The analogs Z3, which is missing a pyrimidine ring N, and ADA in which N in the imidazole ring is shifted, showed lower extents of depurination (Table 1). Since all the A analogs were found to have a reduced rate of MutY catalyzed excision relative to A, decreased acid-catalyzed depurination susceptibility cannot be the only factor leading to poor excision. In fact, even analogs depurinated by acid more readily than A are excised at lower rates. These results indicate that MutY base excision catalysis does not solely rely on susceptibility to protonation of N7 to promote depurination.

These data suggest that efficient base excision by MutY is exquisitely sensitive to the unique structure of A, most likely due to the formation of specific active site contacts (Figure 2c) that “tune” the *N*-glycosidic bond lability and position the substrate base for optimal excision. Notably, due to the low pH and aqueous solutions used in these acid-catalyzed depurination experiments, all protonatable groups of the analogs are likely to be affected,

thus occluding the subtle effects associated with the site-specific protonation on the analogs that would be possible in the MutY active site.

Calculated gas phase acidities of adenine analogs

While the relative experimental susceptibility to acid catalyzed depurination are a measure of the lability of the *N*-glycosidic linkage of the analog within ssDNA in an aqueous solution, the MutY active site provides a more hydrophobic environment with specific contacts that would affect the acidities and proton affinities (PA) of the analogs.³⁵ In order to account for these distinct environments, we calculated the gas-phase acidities of the N9-H and the proton affinities at N7 of each analog using the B3LYP/6-31+G(d) basis set (Figure S5-S8). While these calculations are not a model of the active site, prior studies have shown that gas-phase calculations can be relevant, and lend insight, into reactivity in the non-polar environment of enzyme active sites. Specifically, if the role of a glycosylase is to provide a hydrophobic environment, in which excision depends on the intrinsic lability of the N9-C1' bond, the gas-phase acidities have been shown to track, trendwise, with the rate of excision.³⁵⁻³⁹ Within the active site, multiple contacts are observed between the active site residues and the A substrate such as hydrogen bonds from Arg26 and Glu192 to water to N3 as well as a hydrogen bond from Arg31 to N1 in *Gs* MutY (Figure 2c). Sequence alignments and structural overlay with the *E. coli* MutY N-terminal domain (PDB ID 1MUD) reveal that a majority of these contacts are identical, with the exception of Arg31.⁴⁰ Therefore, we calculated the N9-H acidities for the N7 protonated and N3 hydrogen bonded analogs to model these interactions. The trend for the calculated gas phase acidities (H_{acid} in kcal mol⁻¹) is 2OA-cyto (210.4) > P (214.2) > I (216.3) > BA (218.5) > 2AP (220.6) > A (221.4) > Z3 (223.8) ~ 6mA (223.9) > 2OA (225.6) > ADA (332.7, no N7 to protonate) (Figure S7). Since Z3 has no N3, and 2OA-cyto has a H-bond donor rather than acceptor, the H_{acid} reported for these is the value with the N7 protonated (Figure S6). Furthermore, to evaluate the propensity of the analogs to be protonated within the active site, we calculated the N7 proton affinities (PA) of the analogs. In order of decreasing PA (kcal mol⁻¹), the trend for the analogs is 2AP (221.6) > Z3 (219.8) \approx I (219.6) > 6mA (217.5) > A (215.5) > P (212.7) > 2OA (212.5) > BA (212.0) > 2OA-cyto (209.4) (ADA = no N7 to protonate) (Figure S8). While we observe some broad correlations, H_{acid} and PA largely do not appear to follow the same trends as the rates of excision of the analogs (Figure S2). This observation further substantiates the hypothesis that MutY does not simply depend upon leaving group ability and confirms the identity of the nucleobase within the active site prior to excision.

Strict substrate alignment requirements with MutY catalytic residues for efficient base excision

Closer inspection of the relationship between PA and calculated gas phase acidity, and the MutY base excision rate constant (k_2) revealed additional features imparted in the MutY active site to ensure quality control. Based on the calculated PA of the analogs, the ease with which protonation at N7 takes place is 2AP > Z3 > I > 6mA > A > P > 2OA > BA > 2OA-cyto (ADA has no N7 to protonate) (Figure S8). Since the catalytic mechanism of MutY is dependent upon N7 protonation, analogs that are protonated more easily are expected to be excised faster. While this holds true for a subgroup of the analogs, namely A, P, 2OA and BA, the rates of excision of 2AP, Z3, I and 6mA are not correlated with their PA,

suggesting the influence of additional factors within the active site of MutY (Figure S2). In terms of gas phase acidities of the N7-H and N3 H-bonded analogs, the trend is 2OA-cyto > P > I > BA > 2AP > A > Z3 ~ 6mA > 2OA >> ADA (no N7 to protonate) (Figure S7). In this case as well, we find discrepancies between the acidity of the analogs and k_2 . For instance, the natural substrate, A, is excised fastest by the enzyme despite its midrange acidity. Meanwhile I and BA, calculated to have the highest gas phase acidities, are poorly excised.

If the primary role of the enzyme is to provide an environment to enable the protonation and subsequent cleavage of the base, we would expect the rate of cleavage to follow the same trend as the N9-H acidity with N7 protonated and N3 H-bonded (Figure S7). In prior work with MutY and adenine analogs that were less varied in terms of structure than those studied herein, we did observe this correlation.³⁵ However, since this is not the case with the analogs studied here, we speculate that factors other than intrinsic lability are at play. Specifically, we argue that the formation of contacts between the analog and the active site residues align it with the catalytic residues and influence the rate of cleavage. Numerous contacts between the N1, N3 and the 6-amino group of A with *Gs* MutY active site residues Arg31, Glu192, Arg26, Trp30 and Glu188 have been observed (Figure 2c). We propose that proper engagement of the nucleobase enables rapid alignment with the catalytic residues and results in fast cleavage of the analog. This hypothesis is supported by the PA trend – upon proper alignment with the catalytic Glu, the analog with the highest PA is cleaved fastest. Consequently, the loss of one or more of these contacts negatively impacts the rate of excision of the analog. In the following section we consider the analogs in terms of the structural features they possess and their effects upon alignment within the active site and highlight trends that correlate the acidity with k_2 .

Analogues with N1, N3 and 6-amino (A, BA and ADA)—Within this subgroup, the order of acidity is BA > A > ADA, and A is the only nucleobase efficiently excised by MutY. Based on the ability of these analogs to H-bond to the active site residues, we expect ADA, like A, to be almost perfectly aligned with Glu43. However, the lack of N7 and low N9-H acidity renders ADA resistant to cleavage. In contrast, BA poses a conundrum—while predicted to have a high N9-H acidity (218.5 kcal mol⁻¹), minimal cleavage was observed in one hour. It appears that the steric bulk and electronegativity of the 8-Br group prevents proper alignment of the N7 within the active site, and this feature coupled with its low PA likely conspire to reduce excision.

Analogues with N1 and N3, but missing or modified 6-amino (P, 2AP, 6mA)—In this series, the order of acidity P > 2AP > 6mA is somewhat consistent with the order of excision P > 6mA > 2AP. This correlation further highlights the importance of the fit and alignment of the nucleobase within the active site; in addition to its high N9-H acidity, P lacks any steric or electronic features that may be detrimental to its active site accommodation, retains most of the H-bonding features of A, and has the highest PA among this sub-group. However, the lack of the 6-amino potentially forces the enzyme to sample more conformations to align this nucleobase to the catalytic Glu and Asp, and therefore modestly decreases k_2 compared to A. Meanwhile, 6mA, which only partially loses the

H-bonding capability of the 6-amino group, is excised almost 10-fold faster than 2AP despite its comparatively lower acidity (223.9 kcal mol⁻¹ for 6mA vs 220.6 kcal mol⁻¹ for 2AP), corroborating the above hypothesis and showing that steric bulk at C2 rather than C6 is more detrimental to excision.

Analog with N1 and 6-amino but no N3 (Z3)—Z3 represents one of the most interesting adenine analogs included in this study.²⁹ While its N9-H acidity (223.8 kcal mol⁻¹) is only 2 kcal mol⁻¹ lower than A (221.4 kcal mol⁻¹) and almost identical to 6mA (223.9 kcal mol⁻¹), its rate of excision (0.08 ± 0.01 min⁻¹) is 150-fold lower than A and 5-fold lower than 6mA. If H-bonding to the N3 of A is not considered, the N9-H acidities of A (223.7 kcal mol⁻¹) and Z3 (223.8 kcal mol⁻¹) are essentially identical (Figure S6). H-bonding to the N3 of A increases its acidity and provides contacts within the active site to “lock” the nucleobase into position for protonation and excision. Curiously, though Z3 has a higher PA than A, this factor fails to compensate the absence of N3. In previous analysis of gas phase acidities and k_2 of series of deaza-adenine analogs, we also observed that the higher N9-H acidity of Z3 did not correspond to a higher rate of cleavage.³⁵ Taken together with our present results, these studies corroborate the importance of enzyme-mediated H-bonding to N3 for facile base excision. It is surprising to note that the loss of the single water mediated H-bonding of N3 to Glu192 and Arg26 has a greater negative impact on the rate of excision than the loss of the N1 and 6-amino H bonds.

Analogs with N3 and polarity reversal at N1 (2OA and I)—While I is predicted to be more acidic than canonical 2OA (by ca. 9 kcal mol⁻¹), it is less acidic than 2OA-cyto (by ca. 6 kcal mol⁻¹) (Figure S7). While both these analogs have an H-bonding polarity reversal at N1, the additional polarity reversal at C6 is cumulatively disadvantageous to excision for I (k_2 reduced ~100-fold compared to 2OA). Though the ability of 2OA-cyto to stably H-bond with OG_{anti} (Figure 3) might favor that tautomer in the duplex, it is unknown which tautomer is preferred within the active site. If the predominant tautomer is 2OA-cyto, the trend of excision is readily explained due to its higher acidity; however canonical 2OA possesses the 6-amino and N3, thus contacts with Trp30, Glu188, Glu192 and Arg26 can orient and align it with Glu43 to enable protonation. In fact, the importance of the N3 H-bond highlighted by the Z3 studies suggests that 2OA is the predominant tautomer within the active site. However, in the case of I, the complete polarity reversal at N1 and C6 creates unfavorable contacts within the active site, potentially forcing I into a conformation that misaligns its N7 with Glu43. The fact that I is excised at all by the enzyme may be attributed to its relatively high PA and N9-H acidity.

At this stage, it is interesting to compare the slow excision of I to minimal excision of BA since both these analogs have similarly high N9-H acidities (216.3 kcal mol⁻¹ for I vs 218.5 kcal mol⁻¹ for BA). This discrepancy indicates that bulky substitutions at C8 that affect the fit within the active site are more detrimental to excision than complete polarity reversal of the nucleobase. If the nucleobase analog fits into the active site, the enzyme is capable of stochastically sampling catalytically relevant conformations that allow for proper orientation to protonate N7, and mediate base excision.

Taken together, the observation that even highly labile analogs, based on their calculated PA and N9-H acidities or experimentally determined susceptibility to acid-catalyzed depurination, are not excised at rates higher than A points to two important features of MutY. First, it shows that the active site serves a greater role than simply providing an acidic environment to enable N7 protonation. The sensitivity of k_2 to proper substrate fit in the active site, shows that following recognition of OG:A, MutY further confirms the structure of the A within the active site. Indeed, it appears that the unique structure of A plays as much of a role in “locking” the enzyme into its catalytically competent state as the enzyme plays in orienting the substrate base. This interdependent orientation of active site residues with the substrate ensures that no base other than A is efficiently excised by MutY. Second, with the exception of ADA, BA, and I, which are poor substrates of MutY, complete excision was observed within the hour-long time course of the experiments. This observation highlights that despite being unable to initially align the analog to the catalytic residues, the high affinity afforded by OG provides the opportunity for mutual orientation to enable base excision, indicating that the k_2 of the analogs is limited in part by the enzyme’s stochastic search process of the correct catalytic conformation. Indeed, even ADA and BA were found to be cleaved by MutY after an extended incubation time (Figure S3). These results are in contrast to the catalytic mechanisms employed by other glycosylases, such as TDG and AlkA. For those enzymes, the rate of substrate excision showed a strong correlation to the calculated acidities of the nucleobases.^{37,39,41-43} Since MutY is an unusual glycosylase in that it specifically cleaves the undamaged base paired opposite a lesion, it is crucial for the enzyme to correctly identify both base pairing partners, and therefore it appears to have evolved several structural checkpoints to confirm the structure of the base that is being excised.

The high specificity for cleavage of “A” may prevent excision of improperly placed bases within the MutY active site. For example, the sensitivity of MutY adenine excision to polarity reversal at N1 and C6, and substitution at C2 would prevent excision of G. Similarly, sensitivity of substitution at the 6 and 8 positions of A would prevent excision of natural modified bases 6-methylA and 8-oxoadenine. Though aberrant excision of alternative bases would be expected to be infrequent due to the strong influence of OG upon recognition, these rare events would potentially lead to mutations or strand breaks, thus requiring stringent selection against such inappropriate activity by MutY.

Adenine analogs are repaired to different extents in bacterial cells

To evaluate the impact of the adenine structural modifications on repair in bacterial cells, we performed a cellular repair assay by transforming a plasmid carrying a site-specific OG:Y (Y = A analog) mispair into *muty*⁺ or *muty*⁻ *E. coli* cells. The plasmids were amplified and extracted, and then analyzed by restriction digestion and DNA sequencing to determine the distribution of bps at the lesion site (Figure S10).⁴⁴ In these assays, OG:A lesion bps within the plasmid DNA are fully repaired in the presence of MutY to the correct G:C bps (> 95%), while in the absence of MutY a mixture of G:C and T:A bps are observed at the location of the lesion site (35% G:C, 65% T:A) consistent with equal replication of both bp partners and the expected levels of correct versus mutagenic replication opposite OG.^{26,29} In the absence of MutY, the OG:Y bps containing the A analogs P, 2OA, Z3, 2AP and ADA were processed

similarly to A (~35% G:C) (Table 1). However, higher levels of % G:C were observed with several A analogs indicating altered processing relative to OG:A even in the absence of MutY. Notably, with the OG:I lesion bp high levels of conversion to G:C and detection of C:G in sequencing reactions in *muty*⁻ cells (Table 1, Figure S10) suggests that this analog may be processed by an alternative, MutY-independent repair pathway. I is a natural deamination product of A and its repair is mediated by the glycosylase activity of Mpg and the endonuclease activity of Endo V.⁴⁵⁻⁴⁷ The MutY-mediated repair was quantified as the difference between percent conversion of the OG:Y lesion bp to G:C in plasmids recovered from *muty*⁺ and *muty*⁻ cell lines.⁴⁴ We defined “overall cellular repair” as the normalized value of this difference.

Remarkably, the extent of conversion of all the OG:Y lesion bps to G:C was greater in the presence of MutY and varied considerably within the group of A analogs (Table 1). For ease of discussion, the repair of the A analog bps relative to the natural OG:A substrate are broadly classified into “well repaired” (>60% normalized G:C conversion above background), “moderately repaired” (40-60%) and “poorly repaired” (<40%) categories. By this classification, Z3 and P are “well repaired,” similar to the natural substrate A, whereas BA appears to be “moderately repaired”. 2OA, 6mA, 2AP and ADA are “poorly repaired”, indicating that their specific structure and base pairing to OG results in poor recognition and repair. Notably, within the “poorly repaired” category is OG:I that exhibited an already high level of conversion to G:C in the absence of MutY (Table 1, Figure S10). The observation of MutY mediated repair with all of the A analogs further underscores the heavy reliance of MutY on the presence of OG. These results are consistent with our previous work modifying either OG or the C-terminal domain that illustrated the importance of OG in MutY-mediated cellular repair.^{26,29,48}

Cellular repair by MutY depends upon A analog presentation of the OG_{syn} conformer

To reveal insight into fidelity mechanisms used by MutY, we compared the MutY-catalyzed base excision rate constant k_2 with overall cellular repair of the series of A analogs (Figure 5). Close inspection reveals that k_2 does not have a significant correlation with overall repair. For instance, OG:Z3 bp is repaired to G:C almost as efficiently as OG:A, despite the 150-fold lower k_2 value for base excision in the *in vitro* glycosylase assays. In fact, Z3 is repaired more efficiently than P, where the k_2 is only 2-fold reduced compared to A. However, the other A analogs with k_2 values in the range of Z3 are poorly repaired (2AP, I). The differences between the *in vitro* and cellular experiments are likely a consequence of the more demanding task of lesion bp recognition by MutY in a cellular context where the vast majority of DNA is undamaged. Moreover, repair is in competition with replication and efficient capture of the lesion by MutY is required to prevent mutagenic replication.

We have previously shown that defects in OG recognition by MutY more dramatically reduced OG:A cellular repair than defects in adenine base excision catalysis.^{26,29,48} Indeed, this trend was observed by making specific mutations in MutY, as well as specific modifications of OG. We recently showed that MutY utilizes the major groove 2-amino group of OG as a key detection and recognition feature of OG:A mismatches.^{26,27} The results presented in this work demonstrate the fidelity of MutY for binding and excising

only A, or structures closely resembling A. The fact that T:A or OG:C bps do not present a 2-amino group in the major groove of DNA allows MutY to rapidly bypass these bps and avoid aberrant excision. The unique H-bonding pattern between A and OG stabilizes OG in its *syn* conformation and positions the 2-amino group in the DNA major groove providing a unique structural signature for MutY recognition.

Upon considering the indirect feature of “A” in positioning OG, the results from the cell-based assay are more easily rationalized. Indeed, the A analogs that would be expected to H-bond to OG like A and stabilize the *syn* conformation of OG are repaired most efficiently. The retention of an “A” like Watson-Crick face in Z3, ADA and BA would allow for A-like base-pairing to the N7-H and 6-oxo groups of OG_{*syn*}. This is consistent with duplex stability studies (Table 1, Figure S9) that indicate minimal reduction in stability compared to OG:A (< 4 °C). Despite its low rate of excision, efficient recognition allows Z3 to be repaired in cells. This hypothesis also provides an explanation for the moderate repair observed for BA, and to a lower extent ADA, which are *poorly removed* in our *in vitro* glycosylase assay. The ability of these unnatural base-pairs to be detected provides an opportunity for them to be captured and sequestered from the replication machinery which would create the mutation.

Analogues that are unable to form an “OG_{*syn*}:A_{*anti*}”-like base-pair have reduced levels of overall cellular repair. The analog P has the highest rate of excision among the analogs tested, however, the extent of repair of OG:P is marginally lower than OG:Z3. This may be a consequence of the loss of the H-bond between 6-amino of A and 6-oxo of OG that alters the position of the 2-amino of the OG in the major groove, reducing the efficiency of recognition of OG:P bps by MutY. Interestingly, duplex stability measurements based on DNA melting temperature (T_m), P destabilizes the base pairing with OG ($T_m = -6$ °C) more than 2AP ($T_m = -4$ °C) and 2OA ($T_m = -2$ °C) relative to OG:A. Despite the modest reduction in T_m , the plasmid substrates containing the 2AP and 2OA are poorly repaired by MutY. 2AP may be capable of forming two H-bonds to the 8-oxo and N7-H of OG, but in a fashion that would position the 2-amino group differently in the major groove, thus preventing MutY from “finding” it. The stability of the OG:2OA-containing duplex, and the enthalpy calculations suggest that 2OA prefers the alternative conformation involving the 2OA-cyto tautomer when H-bonding with OG_{*anti*}. In the OG_{*anti*} conformation, positioning the 2-amino group in the minor groove of the helix would lead to complete evasion of recognition by MutY. The reduced stability of the OG:I duplex compared to OG:A ($T_m = -12.8$ C) is similar to introducing a bp mismatch⁴⁹ and may be rationalized by the inability to make complementary H-bonds with OG in its *syn* or *anti* conformation. It is unlikely that the 2-amino group of OG is favorably positioned in the OG:I bp and therefore it eludes detection by MutY. Curiously, these observations indicate that MutY is very specific to the topology of the OG_{*syn*}:A_{*anti*} mispair, such that it completely bypasses a distorted base pair containing OG! These results indicate that within a cellular context, MutY is exquisitely sensitive to the unique structure of OG_{*syn*}:A_{*anti*} to facilitate detection (Figure 6).

CONCLUSIONS

Implications in MutY and MUTYH-mediated repair

MutY-mediated repair of OG:A mismatches is daunting considering the challenge of recognition of a rare lesion in the context of a large excess of structurally similar canonical bps and competition with other cellular processes. The SAR studies herein with A analogs indicate that the identity and presence of a misplaced A base is indirectly detected by MutY via its ability to stabilize the *syn* conformation of OG to display the 2-amino group in the major groove of DNA. This result is consistent with previous work where we showed that the 8OI:A lesion (where 8OI lacks the 2-amino group) is not recognized or repaired at all by cellular MutY.²⁶ The unique ability of A to stably pair with OG in its *syn* conformer prevents MutY from selecting and presenting other bases to its active site such as C from OG:C bps. Furthermore, the detectable levels of repair of the extremely poor processed analogs, BA and ADA, in the cellular assay suggest that by efficiently recognizing and binding the mispair in cells, MutY prevents propagation of T:A mutations. Notably, however, BA and ADA are not repaired as efficiently as the trio of A, P and Z3, indicating that the ability to be efficiently excised by MutY is important for high fidelity repair. The ability of MutY to identify the unique structural features of OG_{*syn*}:A_{*anti*} bps allows for rapid lesion searching with exquisite specificity.

These findings imply that MutY and MUTYH variants that are competent in terms of recognizing and binding the lesion may be able to stall the production of point mutations in cells, despite deficiencies in glycosylase activity. However, abrogation of lesion recognition by MutY variants would be catastrophic even if catalytically competent. This observation is consistent with the consideration that OG:A mismatch detection and repair by MutY must occur rapidly and take place prior to DNA replication to prevent creation of a mutation. Indeed, studies with the bacterial and murine orthologs of the most common MAP variant, Y179C MUTYH (Y82C MutY and Y150C Mutyh), showed that this amino acid substitution had greater impacts upon binding and damage engagement than on the rate of adenine excision.^{18,50-52} In addition, recent studies in our laboratory have shown that a catalytically competent, but recognition deficient MutY variant is incapable of initiating BER in bacterial cells.²⁷ Taken together with our previous SAR study using OG analogs, the work presented herein underscores that importance of chemical confirmation of a lesion as subtle and insidious as OG:A in enabling its repair and preventing mutations. Through this study, we have probed the positions on the adenine bases that tolerate substitution, while maintaining MutY activity. These insights can be used to guide future design of MutY/MUTYH specific probes to monitor the activity, or lack thereof, of MutY/MUTYH variants.⁵³ Moreover, the SAR presented here can be applied towards the development of MutY/MUTYH specific inhibitors that may find utility in cancer therapeutics.⁵⁴⁻⁵⁶

Supplementary Material

Refer to Web version on PubMed Central for supplementary material.

ACKNOWLEDGMENT

The authors gratefully acknowledge the contribution of C. H. McCulley in creating the electrostatic potential maps of the A analogs. We also thank H. R. Vickery and A. K. Marsh for aiding with plasmid extraction for the cell assays. We also thank Tony Francis for providing some initial preliminary results of MutY processing of several A analogs in a different DNA sequence than used herein that provided motivation for more thorough study.

Funding Sources

The work was supported by grants from the NIH CA067985 (S.S.D.) and NSF CHE1761151 (J.K.L.). A.H.M. was a predoctoral trainee supported by T32-GM008799 from NIGMS-NIH. A.H.M. was also supported by GAANN and Corson-Dow fellowships.

LIST OF ABBREVIATIONS

2OA	2-oxoadenine
2OA-cyto	cytosine-like tautomer of 2OA
6mA	6-methyladenine
A	adenine
ADA	7-deaza-8-azadenine
AP	apurinic
BA	8-bromoadenine
8OI	8-oxoinosine
BER	base excision repair
bp	base pair
C	cytosine
dsDNA	double stranded DNA
<i>E. coli, Ec</i>	<i>Escherechia coli</i>
EMSA	electrophoretic mobility shift assay
FA	2'-fluoro-2'-deoxyadenosine
G	guanine
GO	guanine oxidation
<i>Gs</i>	<i>Geobcillus stearothermophilus</i>
HPLC	high-performance liquid chromatography
I	inosine
KIE	kinetic isotope effect
LOVD	Leiden Open Variant Database

MAP	MUTYH associated polyposis
nt	nucleotide
OG	8,oxo,7,8-dihydroguanine
P	purine
PA	proton affinity
PAGE	polyacrylamide gel electrophoresis
RONS	reactive oxygen and nitrogen species
SAR	structure activity relationship
ssDNA	single stranded DNA
T	thymine
T_m	melting temperature
W-C	Watson-Crick
Z3	3-deazadenine

REFERENCES

- (1). Friedberg EC DNA Damage and Repair. *Nature* 2003, 421 (6921), 436–440. 10.1038/nature01408. [PubMed: 12540918]
- (2). Neeley WL; Essigmann JM Mechanisms of Formation, Genotoxicity, and Mutation of Guanine Oxidation Products. *Chem. Res. Toxicol* 2006, 19 (4), 491–505. 10.1021/tx0600043. [PubMed: 16608160]
- (3). McGoldrick JP; Yeh YC; Solomon M; Essigmann JM; Lu AL Characterization of a Mammalian Homolog of the Escherichia Coli MutY Mismatch Repair Protein. *Mol. Cell. Biol* 1995, 15 (2), 989–996. [PubMed: 7823963]
- (4). Banda DM; Nuñez NN; Burnside MA; Bradshaw KM; David SS Repair of 8-OxoG:A Mismatches by the MUTYH Glycosylase: Mechanism, Metals and Medicine. *Free Radic. Biol. Med* 2017, 107, 202–215. <https://doi.org/10.1016/j.freeradbiomed.2017.01.008>. [PubMed: 28087410]
- (5). Drabløs F; Feyzi E; Aas PA; Vaagbø CB; Kavli B; Bratlie MS; Peña-Díaz J; Otterlei M; Slupphaug G; Krokan HE Alkylation Damage in DNA and RNA—Repair Mechanisms and Medical Significance. *DNA Repair (Amst)*. 2004, 3 (11), 1389–1407. <https://doi.org/10.1016/j.dnarep.2004.05.004>. [PubMed: 15380096]
- (6). Tubbs A; Nussenzweig A Endogenous DNA Damage as a Source of Genomic Instability in Cancer. *Cell* 2017, 168 (4), 644–656. <https://doi.org/10.1016/j.cell.2017.01.002>. [PubMed: 28187286]
- (7). Cadet J; Wagner JR TET Enzymatic Oxidation of 5-Methylcytosine, 5-Hydroxymethylcytosine and 5-Formylcytosine. *Mutat. Res. - Genet. Toxicol. Environ. Mutagen* 2014, 764–765, 18–35. 10.1016/j.mrgentox.2013.09.001.
- (8). Locatelli GA; Pospiech H; Tanguy Le Gac N; van Loon B; Hubscher U; Parkkinen S; Syväoja JE; Villani G Effect of 8-Oxoguanine and Abasic Site DNA Lesions on in Vitro Elongation by Human DNA Polymerase ϵ in the Presence of Replication Protein A and Proliferating-Cell Nuclear Antigen. *Biochem. J* 2010, 429 (3), 573–582. 10.1042/BJ20100405. [PubMed: 20528769]

- (9). Maga G; Villani G; Crespan E; Wimmer U; Ferrari E; Bertocci B; Hübscher U 8-Oxo-Guanine Bypass by Human DNA Polymerases in the Presence of Auxiliary Proteins. *Nature* 2007, 447 (7144), 606–608. 10.1038/nature05843. [PubMed: 17507928]
- (10). Briebe LG; Eichman BF; Kokoska RJ; Doublet S; Kunkel TA; Ellenberger T Structural Basis for the Dual Coding Potential of 8-Oxoguanosine by a High-Fidelity DNA Polymerase. *EMBO J* 2004, 23 (17), 3452–3461. 10.1038/sj.emboj.7600354. [PubMed: 15297882]
- (11). Shibutani S; Takeshita M; Grollman AP Insertion of Specific Bases during DNA Synthesis Past the Oxidation-Damaged Base 8-OxodG. *Nature* 1991, 349 (6308), 431–434. 10.1038/349431a0. [PubMed: 1992344]
- (12). Whitaker AM; Smith MR; Schaich MA; Freudenthal BD Capturing a Mammalian DNA Polymerase Extending from an Oxidized Nucleotide. *Nucleic Acids Res.* 2017, 45 (11), 6934–6944. 10.1093/nar/gkx293. [PubMed: 28449123]
- (13). Michaels ML; Cruz C; Grollman AP; Miller JH Evidence That MutY and MutM Combine to Prevent Mutations by an Oxidatively Damaged Form of Guanine in DNA. *Proc. Natl. Acad. Sci* 1992, 89 (15), 7022–7025. [PubMed: 1495996]
- (14). Delaney S; Neeley WL; Delaney JC; Essigmann JM The Substrate Specificity of MutY for Hyperoxidized Guanine Lesions in Vivo. *Biochemistry* 2007, 46 (5), 1448–1455. 10.1021/bi061174h. [PubMed: 17260974]
- (15). Manlove AH; Nuñez NN; David SS The GO Repair Pathway: OGG1 and MUTYH. In *The Base Excision Repair Pathway*; WORLD SCIENTIFIC, 2016; pp 63–115. 10.1142/9789814719735_0003.
- (16). Raetz AG; David SS When You're Strange: Unusual Features of the MUTYH Glycosylase and Implications in Cancer. *DNA Repair (Amst)*. 2019, 80, 16–25. <https://doi.org/10.1016/j.dnarep.2019.05.005>. [PubMed: 31203172]
- (17). Out AA; Tops CM; Nielsen M; Weiss MM; van Minderhout IJ; Fokkema IF; Buisine MP; Claes K; Colas C; Fodde R; Fostira F; Franken PF; Gaustadnes M; Heinemann K; Hodgson SV; Hogervorst FB; Holinski-Feder E; Lagerstedt-Robinson K; Olschwang S; van den Ouweland AM; Redeker EJ; Scott RJ; Vankeirsbilck B; Gronlund RV; Wijnen JT; Wikman FP; Aretz S; Sampson JR; Devilee P; den Dunnen JT; Hes FJ Leiden Open Variation Database of the MUTYH Gene. *Hum Mutat* 2010, 31 (11), 1205–1215. 10.1002/humu.21343. [PubMed: 20725929]
- (18). Al-Tassan N; Chmiel NH; Maynard J; Fleming N; Livingston AL; Williams GT; Hodges AK; Davies DR; David SS; Sampson JR; Cheadle JR Inherited Variants of MYH Associated with Somatic G : C -> T : A Mutations in Colorectal Tumors. *Nat. Genet* 2002, 30 (2), 227–232. 10.1038/Ng828. [PubMed: 11818965]
- (19). David SS; O'Shea VL; Kundu S Base-Excision Repair of Oxidative DNA Damage. *Nature* 2007, 447 (7147), 941–950. 10.1038/Nature05978. [PubMed: 17581577]
- (20). Berti PJ; McCann JAB Toward a Detailed Understanding of Base Excision Repair Enzymes: Transition State and Mechanistic Analyses of N-Glycoside Hydrolysis and N-Glycoside Transfer. *Chem. Rev* 2006, 106 (2), 506–555. 10.1021/cr040461t. [PubMed: 16464017]
- (21). McCann JAB; Berti PJ Adenine Release Is Fast in MutY-Catalyzed Hydrolysis of G:A and 8-Oxo-G:A DNA Mismatches. *J. Biol. Chem* 2003, 278 (32), 29587–29592. 10.1074/jbc.M212474200. [PubMed: 12766151]
- (22). Woods RD; O'Shea VL; Chu A; Cao S; Richards JL; Horvath MP; David SS Structure and Stereochemistry of the Base Excision Repair Glycosylase MutY Reveal a Mechanism Similar to Retaining Glycosidases. *Nucleic Acids Res.* 2016, 44 (2), 801–810. 10.1093/nar/gkv1469. [PubMed: 26673696]
- (23). Fromme JC; Verdine GL Structural Insights into Lesion Recognition and Repair by the Bacterial 8-Oxoguanine DNA Glycosylase MutM. *Nat Struct Biol* 2002, 9 (7), 544–552. 10.1038/nsb809. [PubMed: 12055620]
- (24). Russelburg LP; O'Shea Murray VL; Demir M; Knutsen KR; Sehgal SL; Cao S; David SS; Horvath MP Structural Basis for Finding OG Lesions and Avoiding Undamaged G by the DNA Glycosylase MutY. *ACS Chem. Biol* 2020, 15 (1), 93–102. 10.1021/acscchembio.9b00639. [PubMed: 31829624]

- (25). Wang L; Lee SJ; Verdine GL Structural Basis for Avoidance of Promutagenic DNA Repair by MutY Adenine DNA Glycosylase. *J. Biol. Chem* 2015, 290 (28), 17096–17105. 10.1074/jbc.M115.657866. [PubMed: 25995449]
- (26). Manlove AH; McKibbin PL; Doyle EL; Majumdar C; Hamm ML; David SS Structure-Activity Relationships Reveal Key Features of 8-Oxoguanine: A Mismatch Detection by the MutY Glycosylase. *ACS Chem. Biol* 2017, 12 (9), 2335–2344. 10.1021/acscchembio.7b00389. [PubMed: 28723094]
- (27). Lee AJ; Majumdar C; Kathe SD; Van Ostrand RP; Vickery HR; Averill AM; Nelson SR; Manlove AH; Mccord MA; David SS Detection of OG : A Lesion Mispairs by MutY Relies on Interactions of a Single His Residue with the 2-Amino Group of 8-Oxoguanine. *J. Am. Chem. Soc* 2020, 2–6.
- (28). McAuley-Hecht KE; Leonard GA; Gibson NJ; Thomson JB; Watson WP; Hunter WN; Brown T Crystal Structure of a DNA Duplex Containing 8-Hydroxydeoxyguanine-Adenine Base Pairs. *Biochemistry* 1994, 33 (34), 10266–10270. 10.1021/bi00200a006. [PubMed: 8068665]
- (29). Livingston AL; O’Shea VL; Kim T; Kool ET; David SS Unnatural Substrates Reveal the Importance of 8-Oxoguanine for in Vivo Mismatch Repair by MutY. *Nat. Chem. Biol* 2008, 4 (1), 51–58. 10.1038/Nchembio.2007.40. [PubMed: 18026095]
- (30). Porello SL; Williams SD; Kuhn H; Michaels ML; David SS Specific Recognition of Substrate Analogs by the DNA Mismatch Repair Enzyme MutY. *J. Am. Chem. Soc* 1996, 118 (44), 10684–10692. 10.1021/Ja9602206.
- (31). Chepanoske CL; Porello SL; Fujiwara T; Sugiyama H; David SS Substrate Recognition by Escherichia Coli MutY Using Substrate Analogs. *Nucleic Acids Res.* 1999, 27 (15), 3197–3204. 10.1093/Nar/27.15.3197. [PubMed: 10454618]
- (32). Francis AW; Helquist SA; Kool ET; David SS Probing the Requirements for Recognition and Catalysis in Fpg and MutY with Nonpolar Adenine Isosteres. *J. Am. Chem. Soc* 2003, 125 (52), 16235–16242. 10.1021/Ja0374426. [PubMed: 14692765]
- (33). Nuñez NNNN; Majumdar C; Lay KTKT; David SSSS Chapter Two - Fe–S Clusters and MutY Base Excision Repair Glycosylases: Purification, Kinetics, and DNA Affinity Measurements. In *Fe-S Cluster Enzymes Part B*; David S. S. B. T.-M. in E., Ed.; Academic Press, 2018; Vol. 599, pp 21–68. <https://doi.org/10.1016/bs.mie.2017.11.035>.
- (34). Porello SL; Leyes AE; David SS Single-Turnover and Pre-Steady-State Kinetics of the Reaction of the Adenine Glycosylase MutY with Mismatch-Containing DNA Substrates. *Biochemistry* 1998, 37 (42), 14756–14764. 10.1021/Bi981594+. [PubMed: 9778350]
- (35). Michelson AZ; Rozenberg A; Tian Y; Sun X; Davis J; Francis AW; O’Shea VL; Halasyam M; Manlove AH; David SS; Lee JK Gas-Phase Studies of Substrates for the DNA Mismatch Repair Enzyme MutY. *J Am Chem Soc* 2012, 134 (48), 19839–19850. 10.1021/ja309082k. [PubMed: 23106240]
- (36). Maiti A; Morgan MT; Drohat AC Role of Two Strictly Conserved Residues in Nucleotide Flipping and N-Glycosylic Bond Cleavage by Human Thymine DNA Glycosylase. *J. Biol. Chem* 2009, 284 (52), 36680–36688. 10.1074/jbc.M109.062356. [PubMed: 19880517]
- (37). Morgan MT; Bennett MT; Drohat AC Excision of 5-Halogenated Uracils by Human Thymine DNA Glycosylase - Robust Activity for DNA Contexts Other than CpG. *J. Biol. Chem* 2007, 282 (38), 27578–27586. 10.1074/jbc.M704253200. [PubMed: 17602166]
- (38). Sun X; Lee JK Acidity and Proton Affinity of Hypoxanthine in the Gas Phase versus in Solution: Intrinsic Reactivity and Biological Implications. *J. Org. Chem* 2007, 72 (17), 6548–6555. 10.1021/jo070996x. [PubMed: 17655363]
- (39). Bennett MT; Rodgers MT; Hebert AS; Ruslander LE; Eisele L; Drohat AC Specificity of Human Thymine DNA Glycosylase Depends on N-Glycosidic Bond Stability. *J. Am. Chem. Soc* 2006, 128 (38), 12510–12519. 10.1021/ja0634829. [PubMed: 16984202]
- (40). Guan Y; Manuel RC; Arvai AS; Parikh SS; Mol CD; Miller JH; Lloyd S; Tainer JA MutY Catalytic Core, Mutant and Bound Adenine Structures Define Specificity for DNA Repair Enzyme Superfamily. *Nat Struct Biol* 1998, 5 (12), 1058–1064. 10.1038/4168. [PubMed: 9846876]

- (41). Maiti A; Michelson AZ; Armwood CJ; Lee JK; Drohat AC Divergent Mechanisms for Enzymatic Excision of 5-Formylcytosine and 5-Carboxylcytosine from DNA. *J. Am. Chem. Soc* 2013, 135 (42), 15813–15822. 10.1021/ja406444x. [PubMed: 24063363]
- (42). Michelson AZ; Chen M; Wang K; Lee JK Gas-Phase Studies of Purine 3-Methyladenine DNA Glycosylase II (AlkA) Substrates. *J. Am. Chem. Soc* 2012, 134 (23), 9622–9633. 10.1021/ja211960r. [PubMed: 22554094]
- (43). McKibbin PL; Fleming AM; Towheed MA; Van Houten B; Burrows CJ; David SS Repair of Hydantoin Lesions and Their Amine Adducts in DNA by Base and Nucleotide Excision Repair. *J Am Chem Soc* 2013, 135 (37), 13851–13861. 10.1021/ja4059469. [PubMed: 23930966]
- (44). Majumdar C; Nuñez NNNN; Raetz AGAGAG; Khuu C; David SSSSS Chapter Three - Cellular Assays for Studying the Fe–S Cluster Containing Base Excision Repair Glycosylase MUTYH and Homologs. In *Fe–S Cluster Enzymes Part B*; David S. S. B. T.-M. in E., Ed.; Academic Press, 2018; Vol. 599, pp 69–99. 10.1016/bs.mie.2017.12.006.
- (45). Alseth I; Dalhus B; Bjørås M Inosine in DNA and RNA. *Curr. Opin. Genet. Dev* 2014, 26, 116–123. <https://doi.org/10.1016/j.gde.2014.07.008>. [PubMed: 25173738]
- (46). Saparbaev M; Laval J Excision of Hypoxanthine from DNA Containing DIMP Residues by the Escherichia Coli, Yeast, Rat, and Human Alkylpurine DNA Glycosylases. *Proc. Natl. Acad. Sci. U. S. A* 1994, 91 (13), 5873–5877. [PubMed: 8016081]
- (47). Sebastian Vik E; Sameen Nawaz M; Strøm Andersen P; Fladeby C; Bjørås M; Dalhus B; Alseth I Endonuclease V Cleaves at Inosines in RNA. *Nat. Commun* 2013, 4 (1), 2271. 10.1038/ncomms3271. [PubMed: 23912683]
- (48). Brinkmeyer MK; Pope MA; David SS Catalytic Contributions of Key Residues in the Adenine Glycosylase MutY Revealed by PH-Dependent Kinetics and Cellular Repair Assays. *Chem. Biol* 2012, 19 (2), 276–286. 10.1016/J.Chembiol.2011.11.011. [PubMed: 22365610]
- (49). Kuhn H; Smith DP; David SS Efficient Synthesis of 2'-Deoxyformycin-a Containing Oligonucleotides and Characterization of Their Stability in Duplex DNA. *J. Org. Chem* 1995, 60 (22), 7094–7095. 10.1021/Jo00127a010.
- (50). Livingston AL; Kundu S; Pozzi MH; Anderson DW; David SS Insight into the Roles of Tyrosine 82 and Glycine 253 in the Escherichia Coli Adenine Glycosylase MutY. *Biochemistry* 2005, 44 (43), 14179–14190. 10.1021/Bi050976u. [PubMed: 16245934]
- (51). Nelson SR; Kathe SD; Hilzinger TS; Averill AM; Warshaw DM; Wallace SS; Lee AJ Single Molecule Glycosylase Studies with Engineered 8-Oxoguanine DNA Damage Sites Show Functional Defects of a MUTYH Polyposis Variant. *Nucleic Acids Res.* 2019, 47 (6), 3058–3071. 10.1093/nar/gkz045. [PubMed: 30698731]
- (52). Chmiel NH; Livingston AL; David SS Insight into the Functional Consequences of Inherited Variants of the HMYH Adenine Glycosylase Associated with Colorectal Cancer: Complementation Assays with HMYH Variants and Pre-Steady-State Kinetics of the Corresponding Mutated E.Coli Enzymes. *J. Mol. Biol* 2003, 327 (2), 431–443. 10.1016/S0022-2836(03)00124-4. [PubMed: 12628248]
- (53). Zhu R-Y; Majumdar C; Khuu C; De Rosa M; P. L. Opresko; S. S. David; E. T. Kool Designer Fluorescent Adenines Enable Real-Time Monitoring of MUTYH Activity. *ACS Cent. Sci* 2020, 0 (0). 10.1021/acscentsci.0c00369.
- (54). Gad H; Koolmeister T; Jemth AS; Eshtad S; Jacques SA; Strom CE; Svensson LM; Schultz N; Lundback T; Einarsdottir BO; Saleh A; Gokturk C; Baranczewski P; Svensson R; Berntsson RP; Gustafsson R; Stromberg K; Sanjiv K; Jacques-Cordonnier MC; Desroses M; Helleday T MTH1 Inhibition Eradicates Cancer by Preventing Sanitation of the DNTP Pool. *Nature* 2014, 508 (7495), 215–221. 10.1038/nature13181. [PubMed: 24695224]
- (55). Warpman Berglund U; Sanjiv K; Gad H; Kalderén C; Koolmeister T; Pham T; Gokturk C; Jafari R; Maddalo G; Seashore-Ludlow B; Chernobrovkin A; Manoilov A; Pateras IS; Rasti A; Jemth A-S; Almlöf I; Loseva O; Visnes T; Einarsdottir BO; Gaugaz FZ; Saleh A; Platzack B; Wallner OA; Vallin KSA; Henriksson M; Wakchaure P; Borhade S; Herr P; Kallberg Y; Baranczewski P; Homan EJ; Wiita E; Nagpal V; Meijer T; Schipper N; Rudd SG; Bräutigam L; Lindqvist A; Filppula A; Lee T-C; Artursson P; Nilsson JA; Gorgoulis VG; Lehtiö J; Zubarev RA; Scobie M; Helleday T Validation and Development of MTH1 Inhibitors for Treatment of Cancer. *Ann. Oncol* 2016, 27 (12), 2275–2283. <https://doi.org/10.1093/annonc/mdw429>. [PubMed: 27827301]

- (56). Sharbeen G; Youkhana J; Mawson A; McCarroll J; Nunez A; Biankin A; Johns A; Goldstein D; Phillips P MutY-Homolog (MYH) Inhibition Reduces Pancreatic Cancer Cell Growth and Increases Chemosensitivity. *Oncotarget* 2017, 8 (6), 9216–9229. 10.18632/oncotarget.13985. [PubMed: 27999205]

Author Manuscript

Author Manuscript

Author Manuscript

Author Manuscript

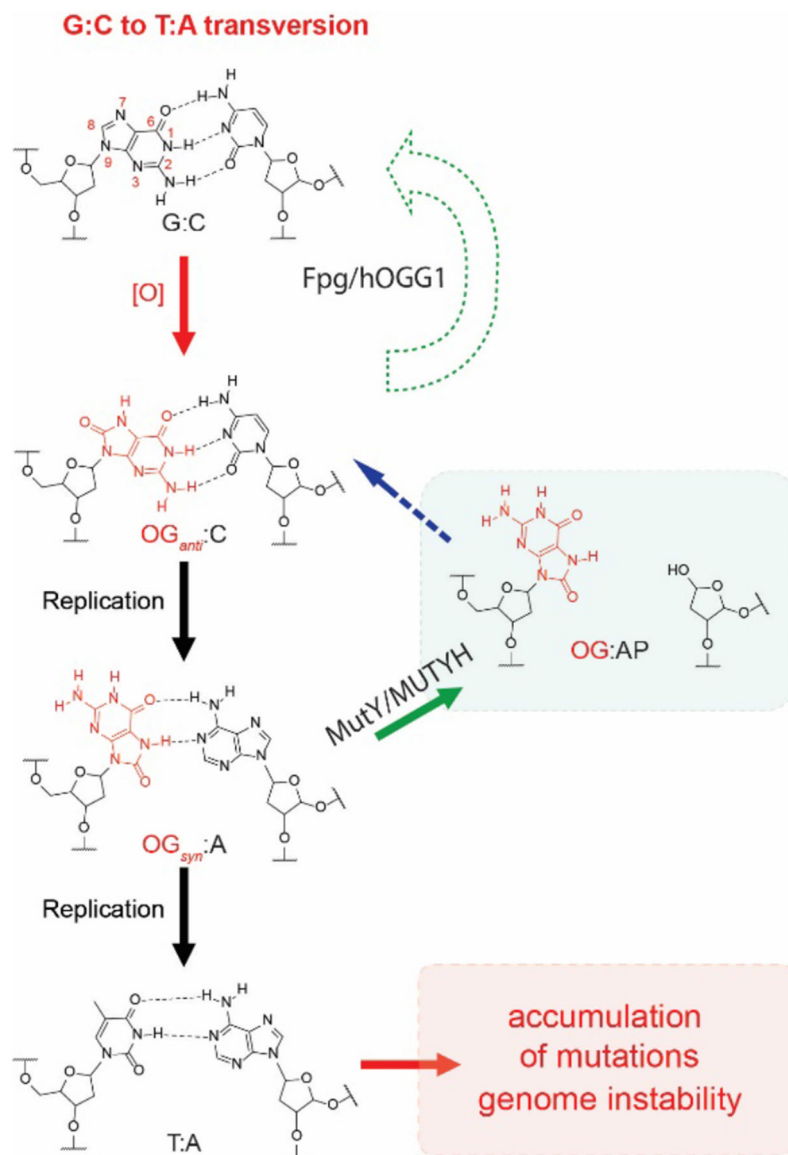


Figure 1. G:C to T:A transversion mutation and ‘GO’ repair pathway.

The BER glycosylases Fpg and MutY act upon their respective base substrates, OG:C and OG:A, and downstream BER enzymes (e.g. AP endonuclease, polymerase, ligase) restore the correct G:C bp.

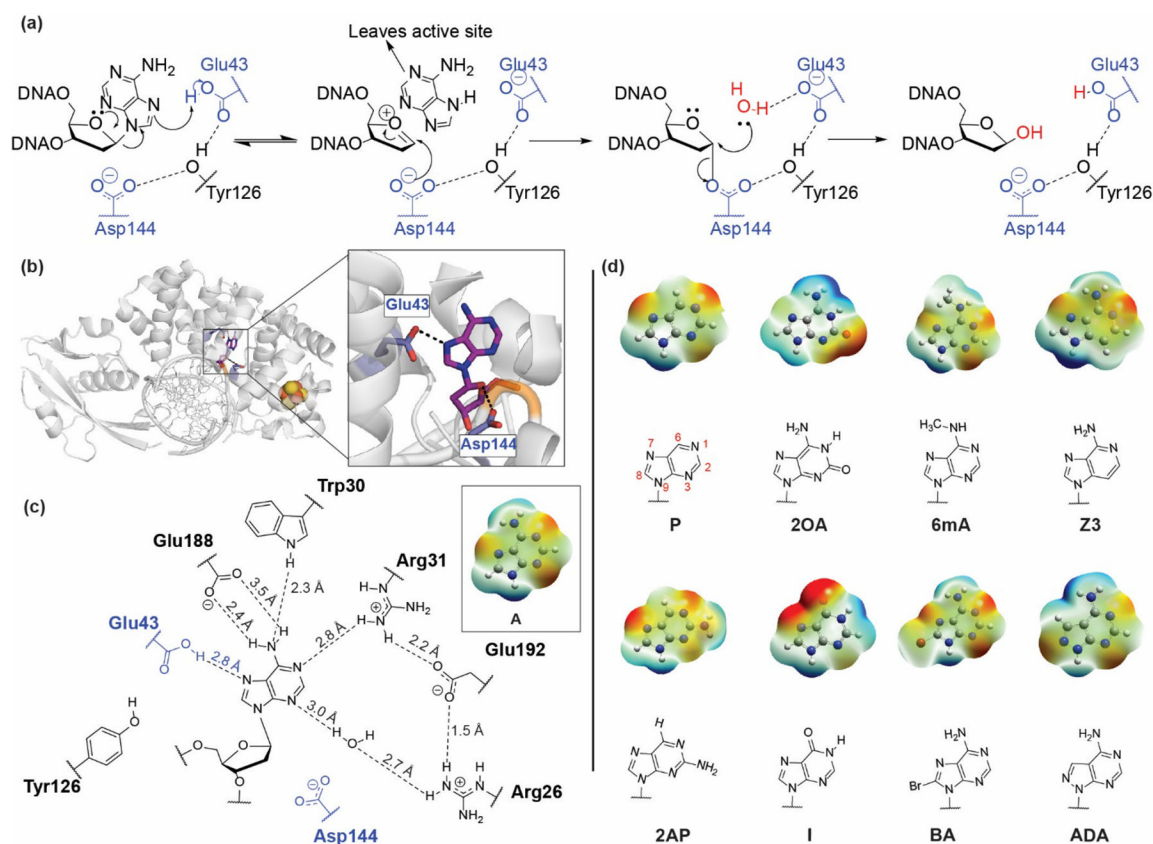


Figure 2. Probing the structural features required for proper A recognition and excision.

(a) Abbreviated mechanism of MutY mediated adenine excision. Protonation of the N7 of A promotes *N*-glycosidic bond scission and departure of A as a neutral leaving group. The resultant oxocarbenium ion is stabilized as a covalent intermediate by Asp144, enabling stereospecific attack by a water molecule to form an abasic site product.²² (b) Crystal structure of *Gs* MutY (gray) bound to the non-cleavable substrate OG:FA showing that within the active site, A (purple) is oriented such that the N7 is aligned with the catalytic Glu43 and the C1' of the sugar is aligned with the catalytic Asp144 (dark blue sticks) (PDB ID: 3G0Q) (c) H-bonding network formed by A with the active site residues; atom numbering on A is shown in red; inset, electrostatic potential map of A. (d) Chemical structures and electrostatic potential maps of the adenine analogs used in this study (isovalue 0.020, density 0.0004).

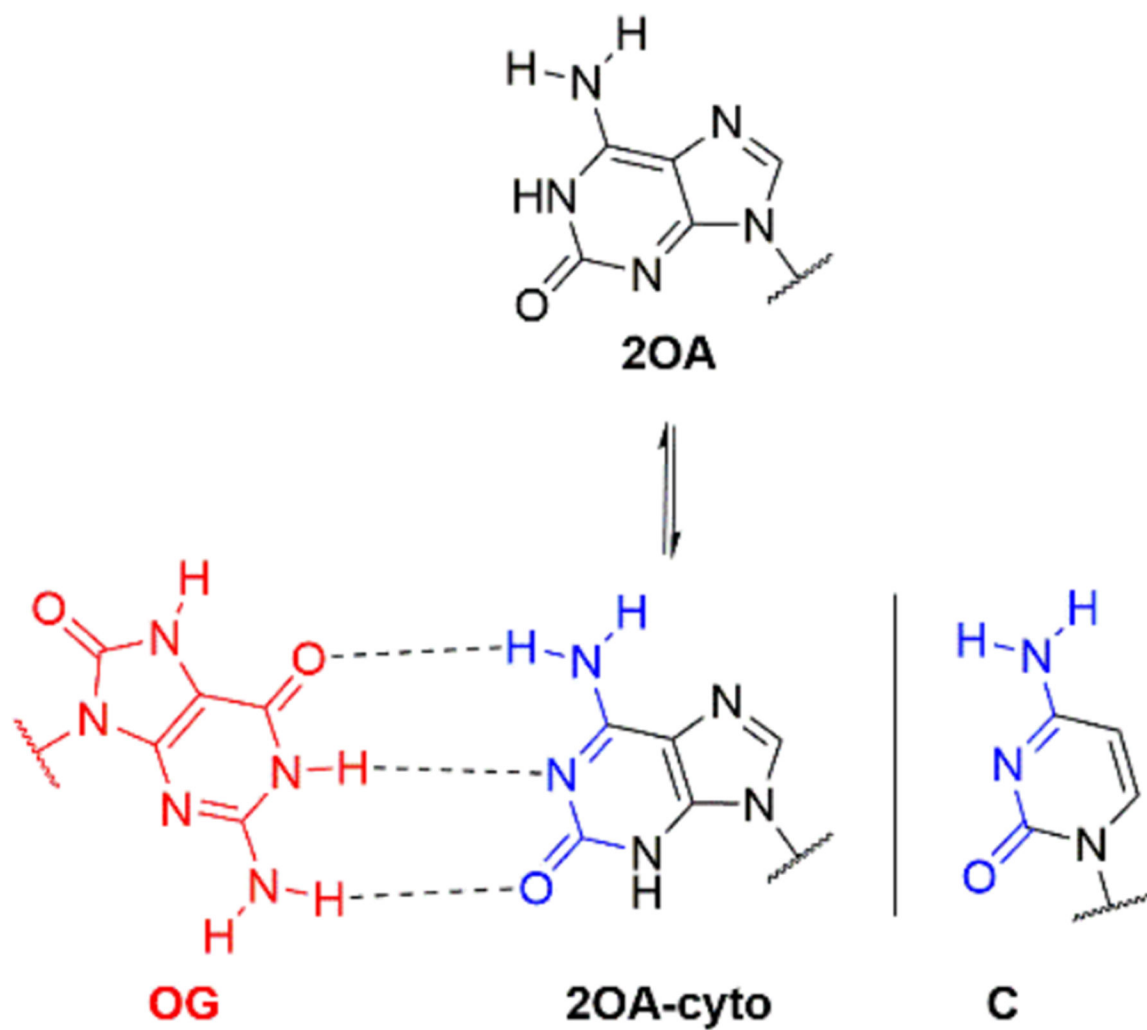


Figure 3. Tautomerization of 2OA to 2OA-cyto can stably base pair with OG_{anti} through a C-like hydrogen bonding face.

The Watson-Crick base pairing face of C and 2OA-cyto are indicated in blue.

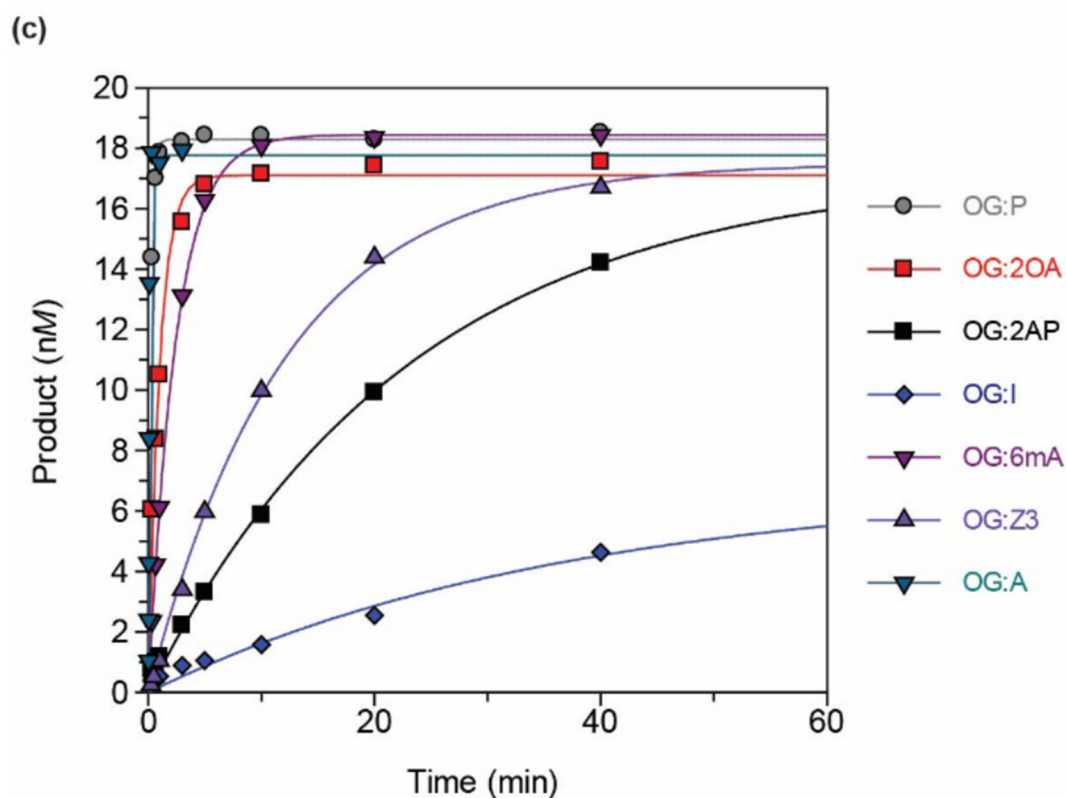
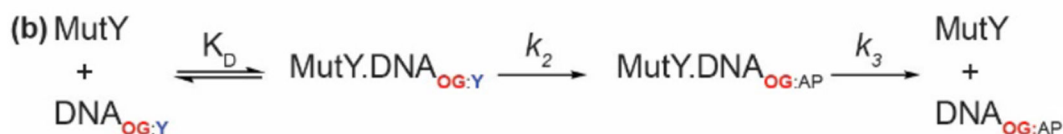


Figure 4. MutY-catalyzed excision of A nucleobase analogs opposite OG in duplex DNA.

(a) 30 bp DNA duplex used for *in vitro* assays (b) Minimal kinetic scheme used to describe MutY processing the OG:Y substrate ($\text{DNA}_{\text{OG:Y}}$) to the abasic site product ($\text{DNA}_{\text{OG:AP}}$), where there are three basic steps, substrate binding (K_D), base excision (k_2) and DNA-product release (k_3). (c) Representative single exponential fits showing time dependent formation of 14 nt product resulting from the removal of A analogs by MutY followed by quenching with 0.2 M NaOH. The experiments were performed under single turnover (STO) conditions at 37°C using 20 nM DNA substrate and 40 nM active WT *E. coli* MutY. The analogs ADA and BA are not plotted as minimal cleavage was observed in the glycosylase assay in 60 minutes.

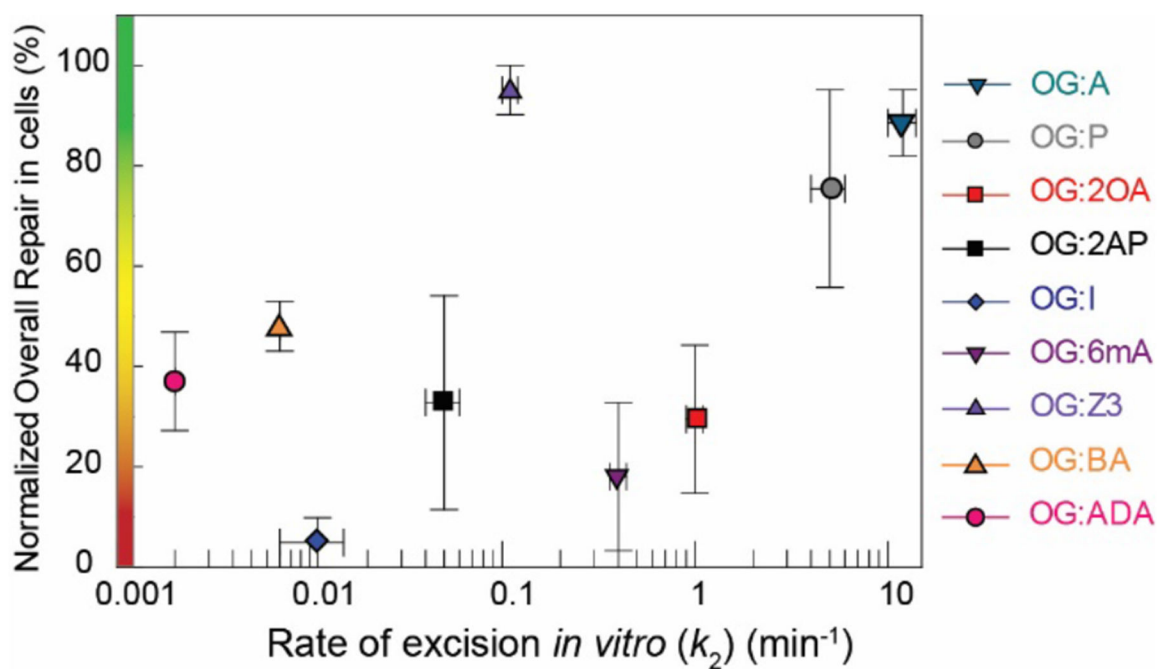


Figure 5. Relationship between overall repair and rate of base excision.

The overall repair plotted on the y-axis represents the normalized percent G:C conversion of each analog in *muty*⁺ cells above background levels in *muty*⁻ cells, as measured by extent of restriction digest by BmtI. The gradient bar indicates the extent of repair ranging from poor (red; <40%), moderate (yellow; ca. 40-60%) to well (green; >60%) repaired.

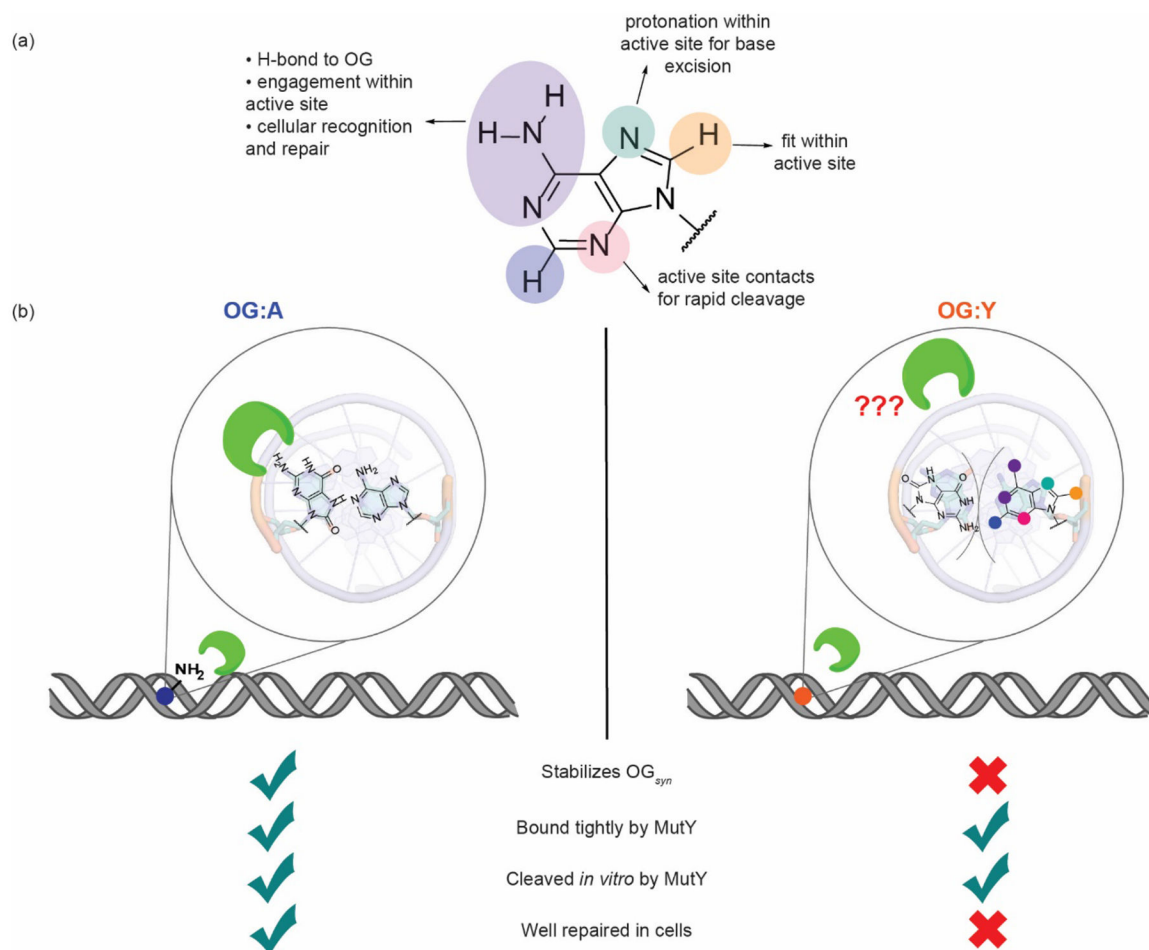


Figure 6. High quality control of MutY engendered at multiple checkpoints.

(a) Summary of SAR highlighting the importance of the different structural features of A in OG:A mismatch recognition and base excision. (b) Positioning of the 2-amino group in the major groove of the helix enables initial recognition of OG:A in a cellular context; left inset, crystal structure of an OG:A mispair (PDB ID 178D) shows that canonical adenine H-bonds with OG and stabilizes the *syn* conformation, which facilitates recognition; right inset, analogs that improperly base pair with OG and displace the 2-amino group from its major groove position leading to inefficient recognition by MutY.

Table 1.

Impact of Adenine analogs on Mut Y binding (Glu37Ser K_D), kinetics of base excision (k_2) and rate of product release (k_3), relative acid lability, duplex stability (T_m) and overall repair in bacterial cells.

Analog	Glu37Ser K _D (nM)	k_2 (min ⁻¹)	k_3 (min ⁻¹)	% G:C in muty ⁺ cells	% G:C in muty ⁻ cells	Acid lability relative to A	T_m (°C)
A	<0.005	12 ± 2	0.002 ± 0.001	92 ± 3	37 ± 3	0.9	71.2 ± 0.3
P	<0.005	5 ± 1	0.005 ± 0.001	80 ± 1	33 ± 8	12	65.2 ± 0.5
2OA	<0.005	1.0 ± 0.1	0.007 ± 0.002	60 ± 10	41 ± 6	6	69 ± 1
6mA	<0.005	0.40 ± 0.04	0.0010 ± 0.004	70 ± 5	58 ± 8	1	68 ± 2
Z3	<0.01 ^a	0.08 ± 0.01 ^a	0.004 ± 0.002 ^a	91 ± 2 ^a	31 ± 2 ^a	0.3 ^a	67 ± 1
2AP	<0.005	0.05 ± 0.01	ND	59 ± 8	38 ± 4	2	66.8 ± 0.7
I	<0.005	0.011 ± 0.004	ND	81 ± 2	77 ± 2	0.9	58.4 ± 0.3
BA	<0.005	<0.007 ^b	ND	78 ± 8	47 ± 1	0.9	70.5 ± 0.8
ADA	<0.005	<0.002 ^b	ND	50 ± 3	27 ± 4	0.5	69.0 ± 0.8

ND: not determined given lack of defined burst phase

^a: Previously reported²⁹

^b: estimated upper limit based on minimal cleavage observed after 1 hr